P4.2

DEPENDENCE OF LONG-TERM TEMPERATURE TRENDS ON WIND AND PRECIPITATION AT URBAN STATIONS IN JAPAN

Fumiaki Fujibe*

Meteorological Research Institute, Tsukuba 305-0052, Japan

1. Introduction

Temperature changes due to urban warming can be a biasing factor in monitoring climate changes, as many observation stations are located at cities and towns. On the global scale, urban warming is believed to be negligible to the observed temperature trend. The IPCC's Fourth Assessment Report (IPCC 2007) has concluded that the global mean temperature trend, estimated to be 0.74°C/century for 1906 to 2005, is little affected by urbanization. Parker (2006, 2010) compared the temperature trends on "windy" and "calm" days at 290 stations in the world, using the NCEP-NCAR reanalysis surface wind data, to define windy and calm weather, and found no significant differences with only a small number of exceptional stations. This fact was interpreted as indicating the insignificance of urban effects on large scale temperature changes, because the urban heat island is generally enhanced on calm nights (e.g., Landsberg 1981; Oke 1987).

On the other hand, studies for some regions including the east Asia have revealed larger temperature trends at urban stations than at rural sites (Zhou et al. 2004; Griffiths et al. 2005; Stone 2007; Hua et al. 2008; Ren et al. 2008; Kataoka et al. 2009; Lai and Cheng 2010; McCarthy et al. 2010). In Japan, urban influence on temperature is quite conspicuous at large cities (Fukui 1957; Kawamura 1985; Fujibe 1995, 2010a; Kato 1996; Ichinose 2003), while urban heat islands have been observed even in small towns and settlements (Tamiya 1968; Tamiya and Ohyama 1981; Sakakibara and Morita 2002). A statistical analysis using data on the AMeDAS (Automated Meteorological Data Acquisition System) network has detected anomalous temperature increase relative to rural sites at stations in areas with population of 100 to 300 people per square kilometer (Fujibe 2009, 2010b), indicating that urban warming is detectable not only in large cities but also at slightly urbanized sites. A signal of urban effect has also been found in the weekly temperature cycle, with lower temperature on Saturdays and holidays than on weekdays (Fujibe 2010a). It is therefore interesting to apply the method of Parker (2006, 2010) to Japan, and to see whether there is any signal indicating urban-induced trend.

The aim of the present study is to detect urban warming in Japan on the basis of dependence on meteorological conditions. It is recognized that the intensity of nocturnal heat island depends not only on wind speed but also on weather, with a larger urban-rural temperature difference under cloudless skies than in cloudy and rainy conditions (e.g., Yamashita et al. 1986; Sakakibara and Matsui 2005). The study therefore evaluates the difference of temperature trends between rainy and non-rainy cases, as well as between windy and calm cases.

2. Data and analysis procedures

2.1 Temperature and population data

The study uses hourly AMeDAS data of temperature, wind and precipitation for 30 years from March 1979 to February 2009. The data are provided with resolution of 0.1°C, 1m/s and 1mm, respectively. The analysis procedure is almost the same as that of Fujibe (2009), except that the period has been extended forward by three years, and that wind and precipitation data have been added for case selection. Stations at which percentage of days with missing data exceeded 3% of the total number of days for any one of the quantities and for any one of the twelve months (for January, for example, days with undefined values were more than 31 days $\times$ 30 years $\times$ 3% = 28) were not used. In order to avoid the influence of discontinuity due to site changes, stations which

* *Corresponding author address:* Fumiaki Fujibe, Meteorological Research Institute, Tsukuba 305-0052, Japan. E-mail: ffujibe@mri-jma.go.jp.

Table 1 List of AMeDAS stations used for analysis.

	Definition or explanation	Number of stations
Large cities	Stations in cities with population of ≥ 500,000.	16
Group A	$P \geq 3000\text{km}^{-2}$, except those in "large cities"	27
Group B	P = 1000–3000km^{-2}.	72
Group C	P = 300–100km^{-2}.	137
Group D	P = 100–300km^{-2}.	110
Reference	P < 100km^{-2}.	142
Total		504

moved by a horizontal distance of 1km or more, or a height of 5m or more, were not used. Figure 1 shows the distribution of 504 stations selected in this way.

The population density around a station i was calculated using the 2000 census data on grids of 30" in latitude and 45" in longitude (about 1km × 1km), applying a weighted average in the form

$$P(i) = \frac{\sum_g \exp\{-(\frac{r_{ig}}{R})^2\}P(g)}{\pi R^2}, \qquad (1)$$

where $P(g)$ is population on the grid g, r_{ig} is its distance from the station i, and R = 3km. Stations were categorized into six groups in P as listed in Table 1. Stations at sites with P <100 km^{-2} were regarded as non-urban and were used as reference stations for defining the urban anomaly.

2.2 Definition of rainy and non-rainy cases

Selection of rainy cases was based on the precipitation data of AMeDAS. However, the 1mm resolution of the data is not sufficient to detect weak precipitation that may affect urban heat budget. The analysis was therefore made using six-hourly precipitation, which was expected to capture weak, continuous precipitation more efficiently than hourly precipitation. A case was regarded as “rainy” if there was ≥ 1mm precipitation for the preceding six hours, and “non-rainy” otherwise. It is to be noted that the term “rainy case” is used symbolically, although it includes some cases of frozen precipitation.

2.3 Definition of windy and calm cases

The analysis was based on surface geostrophic wind speed (GWS) calculated from the sea-level pressure at observatories of the JMA, as an index of the regionally representative wind intensity. Calculation of GWS was made using six-hourly (0300, 0900, 1500, and 2100 JST) data

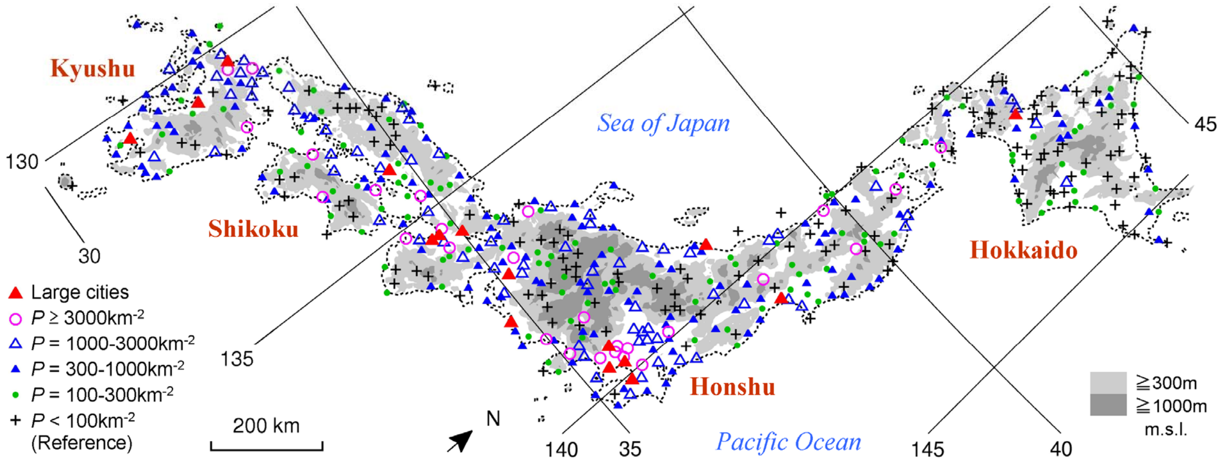

Fig.1 Distribution of AMeDAS stations used in the analysis, and the division of Japan into regions.

at 146 observatories, which were selected on the condition that missing data were less than 100 during the analysis period, based on the least-squares criterion

$$\sum_i \exp\{-(\frac{r_i}{r_G})^2\}\{p_i - (a_i x_i + b_i y_i + c_i)\}^2 \longrightarrow \min., \quad (2)$$

where p_i is sea-level pressure at station i, x_i and y_i are eastward and northward distance from the target point, r_G = 150 km, and a_i and b_i are eastward and northward pressure gradient that were used for calculating GWS. "Windy" and "calm" cases were defined by upper and lower terces, respectively, of GWS at each of the six-hourly observation times during the 30 years. The average values of GWS in windy and calm cases are 9.15m/s and 2.10m/s, respectively. The average GWS over all the cases, namely the annual mean GWS, is 5.29m/s.

2.4 Calculation of urban temperature trends

Hereafter we use the notation $T_{jni}(y)$ to indicate the temperature observed at time j on day n at station i in the year y. The analysis of temperature trend was made using the departure from the climatic mean, $\overline{T_{jni}}$, which was defined for each calendar day as the 30-year average of T_{jni} on that calendar day, with a nine-day running averaging that was applied three times to filter out day-to-day irregularities. The departure from the climatic mean, T^*_{jni}, was then defined as $T^*_{jni}(y) = T_{jni}(y) - \overline{T_{jni}}$.

The average of T^* at non-urban sites surrounding station i was obtained from the least-squares condition:

$$\sum_h \exp\{-(\frac{r_{ih}}{r_0})^2\}[T^*_{jnh} - (a_{jni}x_{ih} + b_{jni}y_{ih} + \tilde{T}^*_{jni})]^2 \longrightarrow \min., \quad (3)$$

where x_{ih} and y_{ih} are respectively the eastward and northward distances from station i of a non-urban station h, $r_{ih}^2 = x_{ih}^2 + y_{ih}^2$, r_0 is a parameter controlling the spatial scale of interpolation, and a_{jni}, b_{jni}, and $\tilde{T}^*_{jni}$, are least-squares coefficients. The value of r_0 was set to 300 km, to ensure that a sufficient number of non-urban stations were included in the calculation. The departure of T^*_{jni} from $\tilde{T}^*_{jni}$, defined as $\delta T^*_{jni}(y) = T^*_{jni}(y) - \tilde{T}^*_{jni}(y)$, was used as the measure of urban anomaly.

The analysis of long-term trend was made after summing $\delta T^*_{jni}(y)$ over days satisfying a specified condition, and stations in a specified group. In order to avoid the influence of seasonal inhomogeniety in number of cases, the summing was first made for each month. For the rainy case, for example,

$$\langle\delta T^*_{mj}(y;\ \text{rainy})\rangle = \sum_{i,n} \delta T^*_{jni}(y)/N, \quad (4)$$

where m is month. The summation in i covers all the stations in the specified region, while the summation in n is for all the days satisfying the specified condition in the month m, and N is the total number of cases covered by these summations. The difference of rainy and non-rainy cases was then obtained by

$$\langle\Delta\delta T^*_{mj}(y;\ \text{RA})\rangle = \langle\delta T^*_{mj}(y;\ \text{rainy})\rangle - \langle\delta T^*_{mj}(y;\ \text{non-rainy})\rangle \quad (5)$$

Likewise, $\langle\delta T^*_{mj}(y)\rangle$ for windy and calm cases, and their difference $\langle\Delta\delta T^*_{mj}(y,\ \text{GWS})\rangle$ was calculated.

Then $\langle\delta T^*_{mj}(y)\rangle$ was smoothed in the way

$$\langle\overline{\delta T}^*_{mj}(y)\rangle = \sum_{j'=j-1}^{j+1} \langle\delta T^*_{mj'}(y)\rangle, \quad (6)$$

or, for the daily mean value of $\langle\delta T^*_{mj'}(y)\rangle$,

$$\langle\overline{\delta T}^*_{m,\text{mean}}(y)\rangle = \sum_{j'=1}^{24} \langle\delta T^*_{mj'}(y)\rangle. \quad (7)$$

The daytime and nighttime mean of $\langle\delta T^*_{mj}(y)\rangle$ was defined by the average for 0700 to 1800 JST, and for 1900 to 0600 JST, respectively.

The linear trend of $\langle\overline{\delta T}^*_{mj}(y)\rangle$ was calculated using the least-squares criterion

$$\sum_{y,m}\{\langle\overline{\delta T}^*_{mj}(y)\rangle - (A_j + T'_j y)\}^2 \longrightarrow \min., \quad (8)$$

where the summation in m covers specified months, and A_j and T'_j are least-squares coefficients. The linear trend is given by T'_j. The same procedure as eqs.(6) to (8) was applied to $\langle\Delta\delta T^*_j\rangle$ to obtain the differential trend between cases. Hereafter we use the notation $\Delta T'_j$ (RA) and $\Delta T'_j$ (GWS) to indicate the differential trend of each parameter.

3. Results

Figure 2 shows the time series of $\langle \delta T^*_{mj}$ (y; rainy)$\rangle$ and $\langle \delta T^*_{mj}$ (y; non-rainy)$\rangle$, and the difference $\langle \Delta\delta T^*_{mj}$ (y; RA)$\rangle$, for the daily mean values at stations in large cities. The time series of $\langle \Delta\delta T^*_{mj}$ (y; RA)$\rangle$ for the nighttime (19–06 JST) is also shown. There is an increasing trend in $\langle \delta T^* \rangle$ both for rainy and non-rainy cases, with a slightly larger value for the former, so that $\langle \Delta\delta T^* \rangle$ has a decreasing trend. Figure 3 shows the time series for windy and calm cases, and their difference. The increase of $\langle \delta T^* \rangle$ is higher for calm cases than for windy cases, so that $\langle \Delta\delta T^*_{mj}$ (y; GWS)$\rangle$ shows a negative trend.

Figure 4 shows the annually averaged values of T'_j (non-rainy and rainy) and $\Delta T'_j$ (RA) for each population group. Figure 5 shows those of T'_j (calm and windy) and $\Delta T'_j$ (GWS). Generally T'_j is positive, and tends to be larger for groups with larger values of P. This fact indicates that urban signal is detectable both in non-rainy and rainy conditions, and in calm and windy conditions. However, $\Delta T'_j$ (RA) is significantly negative for all the station groups including that for $100 \leq P < 300$ km^{-2}, indicating that urban warming is more conspicuous under non-rainy conditions than in rainy conditions not only in large cities but also at slightly populated sites. For $\Delta T'_j$ (GWS), significant negative values are found for stations in large

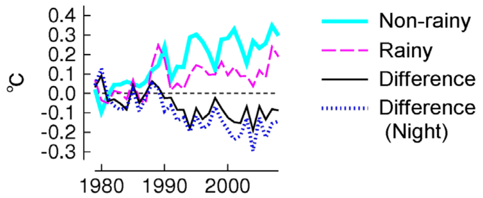

Fig.2 Time series of δT^* for non-rainy and rainy cases (daily mean), and their difference $\Delta\delta T^*$ (daily and nighttime mean) for stations in large cities, based on an analysis covering the whole year and whole country.

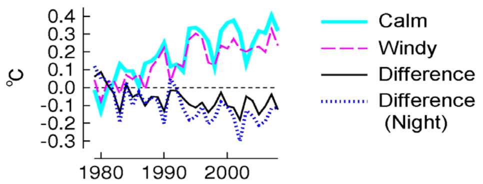

Fig.3 Same as Fig.2, but for calm and windy cases.

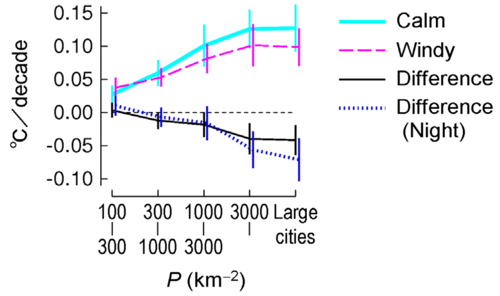

Fig.4 Dependence of T' for non-rainy and rainy cases (daily mean), and their differential trend $\Delta T'$ (daily and nighttime mean) on categories of population density, P. Vertical bars indicate 95% confidence ranges.

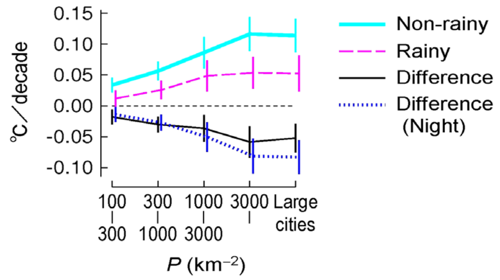

Fig.5 Same as Fig.4, but for calm and windy cases.

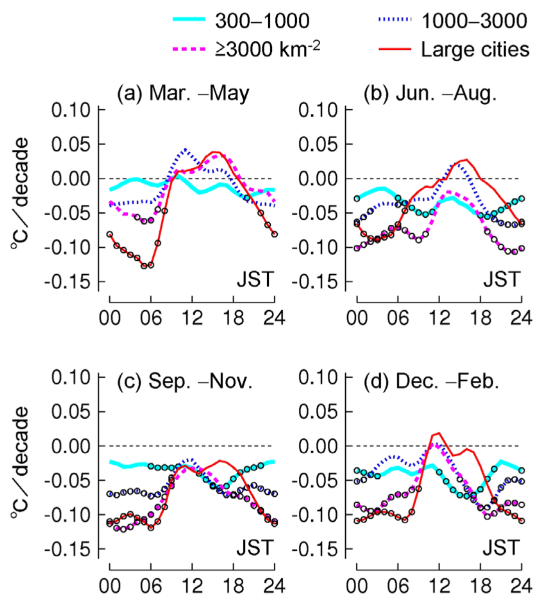

Fig.6 Time-of-day dependence of $\Delta T'$ (RA) for each category of population density, P, and season.

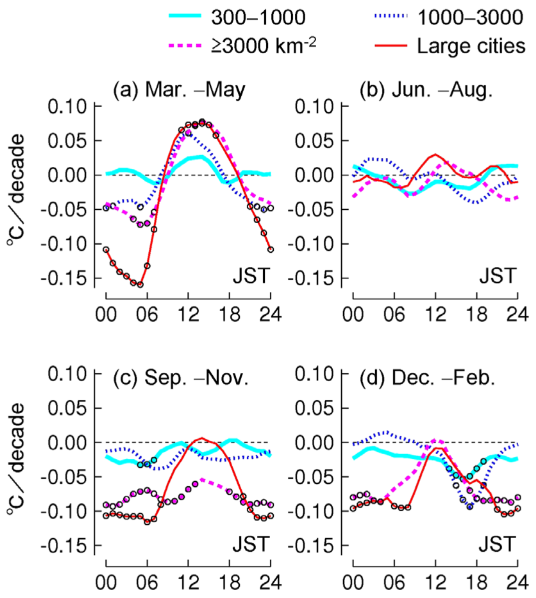

Fig.7 Same as Fig.6, but for $\varDelta T'$ (GWS).

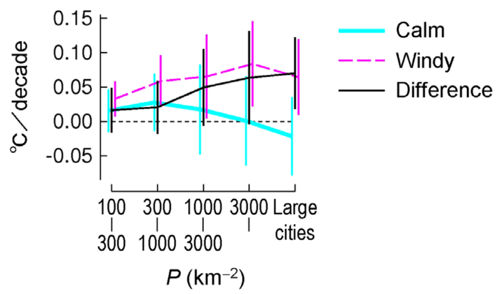

Fig.8 Same as Fig.5, but for the daytime (10-15 JST) of spring (March-May).

cities and the $P \geq 3000$ km^{-2} group. Negative values of $\varDelta T'_j$ tend to be larger in the nighttime than for the daily mean, in agreement with our general understanding that urban warming is more conspicuous in the nighttime than in the daytime.

Figure 6 shows the diurnal variation of $\varDelta T'_j$ (RA) for each season (for simplicity, results for $100 \leq P < 300$ km^{-2} stations are not shown). In all the seasons, $\varDelta T'_j$ (RA) has significant negative values at night or at least part of the night, while it is generally small in the daytime. A similar diurnal variation pattern is observed for $\varDelta T'_j$ (GWS) in winter (Fig.7). For large cities, significant negative values of $\varDelta T'_j$ (GWS) are also found in spring and autumn, although no difference is found for summer.

An exceptional feature in Fig.7 is the positive $\varDelta T'_j$ (GWS) values in the daytime of spring at stations in groups $P \geq 1000$ km^{-2}. Figure 8 shows T'_j (GWS) and $\varDelta T'_j$ (GWS) for the midday of spring (10-15 JST from March to May). There are positive trends ($T'_j > 0$) in windy cases, while calm cases show no significant trends that tend to decrease with P, so that $\varDelta T'_j$ has significant positive values for stations in large cities and the $P \geq 3000$ km^{-2} group. The $\varDelta T'_j$ value for stations in the $1000 \leq P < 3000$ km^{-2} group is also significant at the 10% level.

4. Concluding remarks

The present study has revealed higher urban warming, which was defined by the trend of temperature departure from rural sites, in non-rainy cases than in rainy cases even for slightly urbanized sites with population density of $100 \leq P < 300$ km^{-2}. For the difference between windy and calm cases, higher trends in calm cases are found for stations with population density of $P \geq 3000$ km^{-2}. Both the rainy versus non-rainy difference and the windy versus calm difference are more conspicuous for the nighttime temperature than the daily mean. These features agree with our understanding that urban temperature anomaly is enhanced in the nighttime under calm and cloudless conditions. In this respect, the present study has given convincing evidence of urban warming in Japan, not only in large cities but also at slightly urbanized sites. This result is in agreement with the previous finding of anomalous trends and weekday-weekend differences in urban temperature in Japan (Fujibe 2009, 2010a,b).

Acknowledgments

This work was partly supported by Grant-in-Aid from the Japan Society for the Promotion of Science (No. 22340141, 2010–2012).

References

Fujibe, F., 1995: Temperature rising trends at Japanese cities during the last hundred years and their relationships with population, population increasing rates and daily temperature ranges. *Pap. Meteor. Geophys.*, **46**, 35-55.

Fujibe, F., 2009: Detection of urban warming in recent temperature trends in Japan. *Int. J.*

Climatol., **29**, 1811-1822.
Fujibe, F., 2010a: Day-of-the-week variations of urban temperature and their long-term trends in Japan. *Theor. Appl. Climatol.*, Online First, doi: 10.1007/s00704-010-0266-y.
Fujibe, F., 2010b: Urban warming in Japanese cities and its relation to climate change monitoring. *Int. J. Climatol.*, Early View, doi: 10.1002/joc.2142.
Fukui, E., 1957: Increasing temperature due to the expansion of urban areas in Japan. *J. Meteor. Soc. Japan*, 75th anniversary volume, 336-341.
Griffiths, G. M., L. E. Chambers, M. R. Haylock, M. J. Manton, N. Nicholls, H.-J. Baek, Y. Choi, P. M. Della-Marta, A. Gosai, N. Iga, R. Lata, V. Laurent, L. Maitrepierre, H. Nakamigawa, N. Ouprasitwong, D. Solofa, L. Tahani, D. T. Thuy, L. Tibig, B. Trewin, K. Vediapan and P. Zhai, 2005: Change in mean temperature as a predictor of extreme temperature change in the Asia-Pacific region. *Int. J. Climatol.*, **25**, 1301-1330.
Hua, L. J., Z. G. Ma and W. D. Guo, 2008: The impact of urbanization on air temperature across China. *Theor. Appl. Climatol.*, **93**, 179-194.
Ichinose, T., 2003: Regional warming related to land use change during recent 135 years in Japan. *J. Global Environ. Eng.*, **9**, 19-39.
IPCC, 2007: *Climate Change 2007: The Physical Science Basis. Contribution of Working Group I to the Fourth Assessment Report of the IPCC*. S. Solomon et al. eds, Cambridge University Press, New York, 1056pp.
Kataoka, K., F. Matsumoto, T. Ichinose and M. Taniguchi, 2009: Urban warming trends in several large Asian cities over the last 100 years. *Sci. Total Environ.*, **407**, 3112-3119.
Kato, H., 1996: A statistical method for separating urban effect trends from observed temperature data and its application to Japanese temperature records. *J. Meteor. Soc. Japan*, **74**, 639-653.
Kawamura, T., 1985: Recent changes of atmospheric environment in Tokyo and its surrounding area. *Geogr. Rev. Japan*, **58B**, 83-94.
Lai, W.-L. and W.-L. Cheng, 2010: Air temperature change due to human activities in Taiwan for the past century. *Int. J. Climatol.*, **30**, 432-444.
Landsberg, H. E., 1981: *The Urban Climate*. Academic Press, 275pp.
McCarthy, M. P., M. J. Best and R. A. Betts, 2010: Climate change in cities due to global warming and urban effects. *Geophys. Res. Lett.*, **37**, L09705, doi:10.1029/2010GL042845.
Oke, T. R., 1987: *Boundary Layer Climates*. 2nd ed., Methuen, Co. Ltd., London, 435pp.
Parker, D. E., 2006: A demonstration that large-scale warming is not urban. *J. Climate*, **19**, 2882-2895.
Parker, D. E., 2010: Urban heat island effects on estimates of observed climate change. *Wiley Interdiscip. Rev. Clim. Change*, **1**, 123-133.
Ren, G. Y., Y. Zhou, Z. Chu, J. Zhou, A. Zhang, J. Guo and X. Liu, 2008. Urbanization effects on observed surface air temperature trends in North China. *J. Climate*, **21**, 1333-1348.
Sakakibara, Y. and E. Matsui, 2005: Relation between heat island intensity and city size indices/urban canopy characteristics in settlements of Nagano basin, Japan. *Geogr. Rev. Japan*, **78**, 812-824.
Sakakibara, Y. and A. Morita, 2002: Temporal march of the heat island in Hakuba, Nagano. *Tenki*, **49**, 901-911 (in Japanese with English abstract).
Stone, B. Jr., 2007: Urban and rural temperature trends in proximity to large US cities: 1950-2000. *Int. J. Climatol.*, **27**, 1801-1807.
Tamiya, H., 1968: Night temperature distribution in a new-town, western suburbs of Tokyo. *Geogr. Rev. Japan*, **41**, 695-703 (in Japanese with English abstract).
Tamiya, H. and H. Ohyama, 1981: Nocturnal heat island of small town, its manifestation and mechanism. *Geogr. Rev. Japan*, **54**, 1-21 (in Japanese with English abstract).
Yamashita, S., K. Sekine, M. Shoda, K. Yamashita and Y. Hara, 1986: On relationships between heat island and sky view factor in the cities of Tama River basin, Japan. *Atmos. Environ.*, **20**, 681-686.
Zhou, L., R. E. Dickinson, Y. Tian, J. Fang, Q. Li, R. K. Kaufmann, C. J. Tucker and R. B. Myneni, 2004: Evidence for a significant urbanization effect on climate in China. *Proc. Natl. Acad. Sci.*, **101**, 9540-9544.